IEEE Access
Multidisciplinary ⋮ Rapid Review ⋮ Open Access Journal

Received October 20, 2019, accepted December 1, 2019, date of publication December 6, 2019, date of current version December 23, 2019.

Digital Object Identifier 10.1109/ACCESS.2019.2958050

High-Gain Wideband Metasurface Antenna With Low Profile

HAO BAI[1], GUANG-MING WANG[1], AND TING WU[2]

[1]Air-Defense and Antimissile Institute, Air Force Engineering University, Xi'an 710051, China
[2]Automation and Information Engineering Institute, Xi'an University of Technology, Xi'an 710048, China

Corresponding author: Guang-Ming Wang (wgming01@sina.com)

This work was supported in part by the National Natural Science Foundation of China under Grant 61871394, in part by the Program for Talent of Colleges and Universities Service Enterprise of Xi'an under Grant 201805037YD15CG21 (10), in part by the Program for Science and Technology Innovation of Xi'an University of Technology under Grant 103-256081703, and in part by the Xi'an Beilin District Science and Technology Plan under Grant GX1920.

ABSTRACT In this paper, a novel compact wideband and high-gain antenna based on metasurface is proposed. The antenna is an octagon with a side length of 32.3 mm and a height of 5.6 mm. The metasurface consists of two stacking layers, and both layers contain a 4×4 copper patch array. The antenna is excited by an aperture coupled structure made of an anomalous microstrip line and a narrow slot etched in the ground plane. Genetic algorithm (GA) is adopted to optimize all the parameters and obtain the valid performance of the metasurface antenna. Moreover, the antenna is modified by introducing nonuniform patch. Modification leads to varying degrees gain enhancement, and the peak is approximately 1.5 dB at 6.1GHz. The impedance bandwidth of the proposed antenna is 54.9%, ranging from 4.48–7.87 GHz. A prototype of the antenna is fabricated, and the measured results verify the design.

INDEX TERMS Wideband, metasurface, optimization algorithm, nonuniform patch, high gain.

I. INTRODUCTION

With the increasing demands for high speed and large channel capacity in modern mobile communication systems, broadband and high-gain antenna technologies have been rapidly developed [1]–[3]. There are many high-gain antennas, such as waveguide antennas [4], [5], lens antennas [6]–[8], and planar antennas [9], [10]. High-gain waveguide and lens antennas are very large and thus inappropriate for miniaturization and system-level integration. Planar antennas have been widely used in various wireless communications systems due to their low profiles, easy integration, and low fabrication costs [11]. However, the gain and bandwidth of traditional patch antennas are limited. For patch antenna arrays, dielectric losses increase with the operating frequency, which limits their practical applications.

Currently, researchers are studying a new kind of antenna called metasurface antenna. Metasurface antennas have been used to reduce the antenna profile, enlarge the operating band, and improve the directivity of the antenna [12]–[14]. Metasurfaces are very universal and have drawn increasing attention in the past few years [15]–[18]. In [19], a wideband directive metasurface with aperture coupling feeding was proposed. In [20], a metasurface was formed by an array of mushroom cells, and the antenna obtained a 25% impedance bandwidth with a 9.9-dBi peak gain. In [12], a single layer of a periodic array of patch cells formed the metasurface. The antenna had a 28% impedance bandwidth and a maximum gain of 9.8 dBi. We can see that the impedance bandwidth of the metasurface antennas listed above is no more than 30%. In [21], a wideband, low-profile antenna loaded with a dual-layer metasurface was proposed. The 10-dB impedance bandwidth of the proposed antenna was approximately 44% (4.08–6.38 GHz). However, the gain of the proposed antenna was not very steady. The gain increases gradually from 7 dB to 12 dB, and then decreases rapidly to 7.5 dB, which means that the value of the gain does not remain stable. To improve the gain of the antenna, various methods have been reported, such as complemental boundaries [11] and parasitic elements [22]. These methods have proven to be efficient.

In this paper, we propose a novel compact high-gain metasurface antenna with an improved impedance bandwidth. The simulated results show that the impedance bandwidth of the proposed antenna is 54.9% from 4.48–7.87 GHz.

The associate editor coordinating the review of this manuscript and approving it for publication was Andrei Muller.

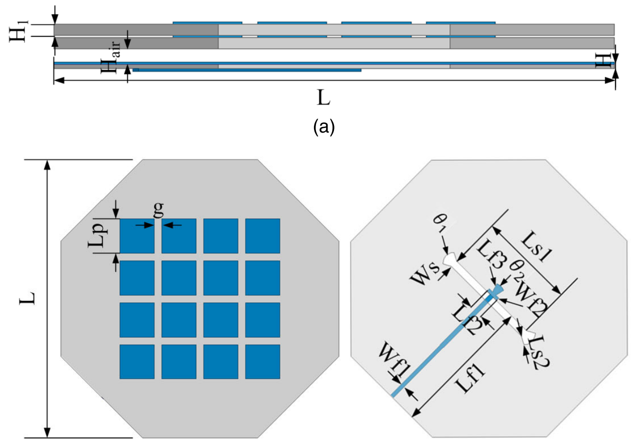

FIGURE 1. Configuration of the proposed antenna. (a) Side view of the metasurface. (b) Top view of the metasurface. (c) Top view of the feeding layer.

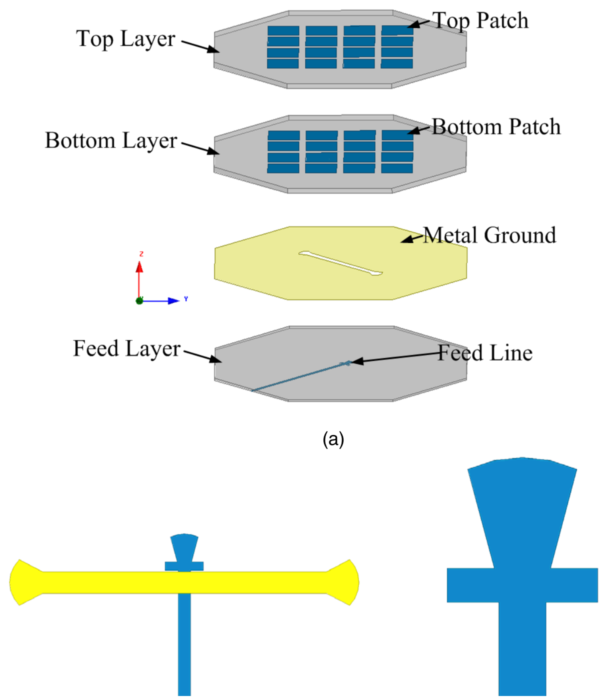

FIGURE 2. Stereograms of the antenna. (a) Expanded structure of the antenna. (b) Feeding structure. (c) Anomalous microstrip line.

Compared with the design in [21], our antenna has good stability. The variation of the gain is 1.7 dB in the frequency band from 4.48–6 GHz, while it is 1.5 dB in the frequency band from 6–7.87 GHz. The measured variation of the gain in the working band is 3 dB. We adopt the genetic algorithm (GA) to obtain the valid performance of the metasurface antenna. Moreover, the gain is enhanced by introducing nonuniform patch (NP) while keeping the other parts of the antenna fixed. The paper includes four parts. In section II, we discuss the design and optimization of the proposed antenna. Then, the experimental results and discussion are presented in section III. Finally, the work is concluded in section IV.

II. DESIGN AND OPTIMIZATION OF THE PROPOSED ANTENNA

A. STRUCTURE OF THE ANTENNA

Figure 1 shows the structure of the proposed metasurface antenna. The proposed antenna is an octagon due to the limitation of the installation platform. The side view of the antenna is shown in Figure 1 (a), revealing two stacking layers and a ground plane. As shown in Figure 1 (b), two layers of the same size constitute the metasurface. Each layer contains a copper patch array printed on an F4B substrate with a thickness of $H_1 = 1.5$ mm, relative permittivity of $\varepsilon_r = 2.65$, and loss tangent of 0.002. The patch array is formed by 4×4 copper cells uniformly distributed along the x and y directions, with a gap width g. From Figure 1 (c), we can see that the metasurface antenna is excited by the aperture coupled structure, which is placed underneath the metasurface. The structure is made of an anomalous microstrip line and a narrow slot etched in the ground plane. In this way, two adjacent resonance modes can be excited simultaneously. The feeding part is fabricated on an F4B substrate with a thickness of $H = 0.6$ mm, relative permittivity of $\varepsilon_r = 2.65$, and loss tangent of 0.002. The proposed antenna is simulated and studied by the high-frequency structure simulator (HFSS).

Stereograms of the antenna structure are shown in Figure 2. The antenna consists of three stacking layers. The top patch is etched on the upper surface of the top layer, and the bottom patch is etched on the upper surface of the bottom layer. The metal ground is etched on the upper surface of the feed layer while the feed line is etched on the lower surface, as shown in Figure 2(a). The feeding structure is shown in Figure 2(b). As shown in Figure 2(c), the anomalous microstrip line is composed of a scallop and a branch to improve matching. The overall dimension of the antenna is $2.04\lambda_0 \times 2.04\lambda_0 \times 0.16\lambda_0$ (λ_0 is the operating wavelength in free space).

As seen from the above description, the metasurface consists of two stacking layers of the same size. In addition, each layer contains a uniformly distributed copper patch array. The orientation of the 4×4 copper cells in the first and the second layers affects the performance of the antenna. To better understand the influence of the orientation, we simulated four antennas with different orientations. The antennas are called antenna 1, antenna 2, antenna 3, and antenna 4, as shown in Figure 3. The simulated S_{11} of each antenna is shown in Figure 4. We can see that the impedance bandwidth of antenna 1 is the widest of the four antennas. Therefore, we choose antenna 1 for further study.

B. PARAMETRIC STUDY

In this part, some critical parameters are studies to analyze that ones can influence the performance of the antenna. In the simulation, we found that some of the parameters greatly

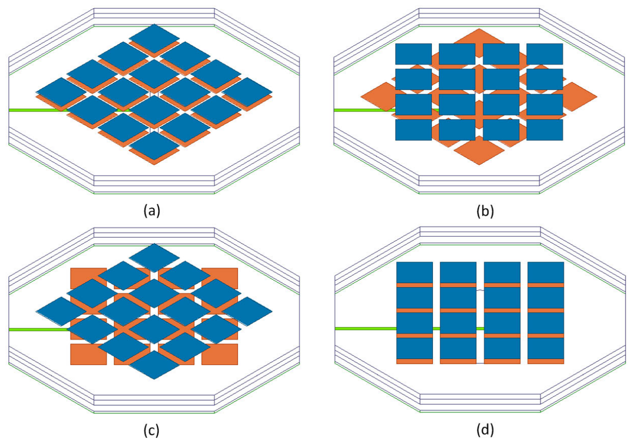

FIGURE 3. Different combinations of antennas. (a) Antenna 1. (b) Antenna 2. (c) Antenna 3. (d) Antenna 4.

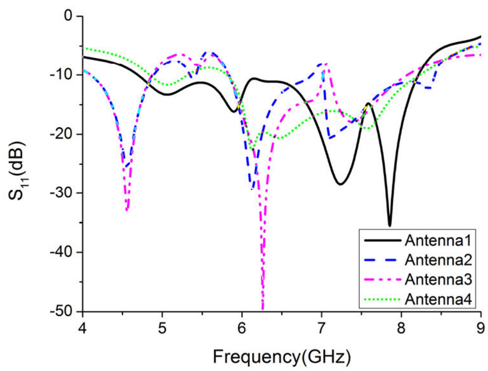

FIGURE 4. Simulated S_{11} of each antenna.

influence the performance of the antenna; thus, they are typically. Through the changes of these parameters, we can seek a rule that will lay the foundation for the optimization and simplification of the antenna design in the next step. First, the effects of unit cell size on impedance performance are shown in Figure 5. L_p is the side length of the square cell, which we change from 8 to 10 mm. It can be seen that, when $L_p = 9$ mm, the antenna has the widest impedance bandwidth; thus, in this paper, we set $L_p = 9$ mm. Then, the effects of different gap widths g in the patch array are studied. As seen from Figure 6, the first resonance obviously moves to a higher frequency when g increases. This phenomenon occurs because the equivalent capacitance decreases as the gap width g increases. When g = 2 mm, the antenna has the widest impedance bandwidth.

The proposed metasurface antenna is excited by the aperture coupled structure, which is made of an anomalous microstrip line and a narrow slot etched in the ground plane. The dimensions of the slot greatly influence the antenna. We change the distance from the feeding port to the coupling slot Lf1 while keeping the other parameters fixed. It can be seen from Figure 7 that, when Lf1 = 37.5 mm, the antenna can achieve the widest impedance bandwidth. The effects of different widths of the coupling slot Ws are also studied

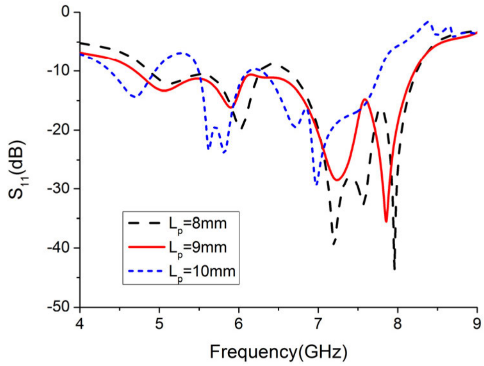

FIGURE 5. Effect of L_p on the performance of the proposed antenna.

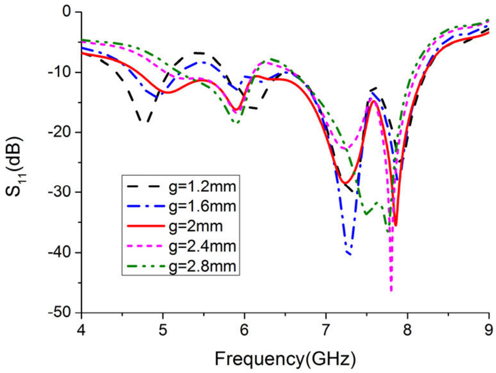

FIGURE 6. Effect of g on the performance of the proposed antenna.

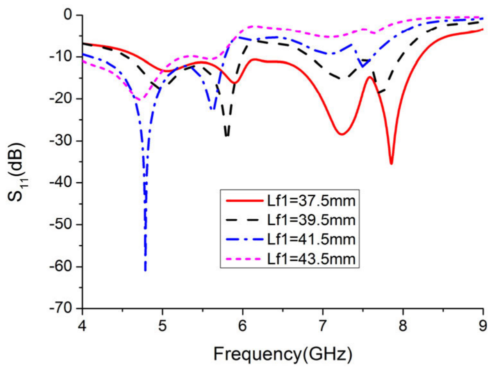

FIGURE 7. Effect of Lf1 on the performance of the proposed antenna.

in Figure 8. It is shown that the impedance bandwidth is widest when Ws = 2 mm. To further improve the performance of the antenna, a minor modification is made to the both ends of the coupling slot. The length of the sector end Ls2 changes from 0.5 to 4.5 mm, and we can see from Figure 9 that the impedance bandwidth is widest when Ls2 = 2.5 mm. In addition, the distance between the metasurface and the ground plane H_{air} also affects the performance of the antenna. As shown in Figure 10, the high working band improves and the low working band worsens as H_{air} increases. We choose $H_{air} = 2$ mm to obtain the best performance in the impedance bandwidth.

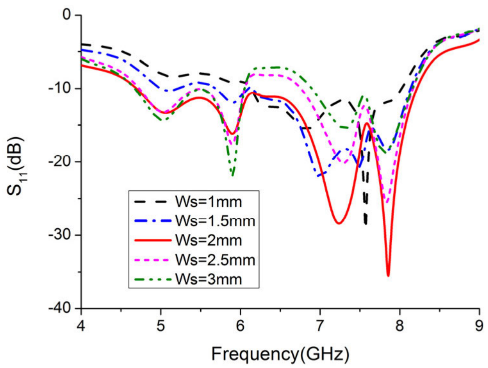

FIGURE 8. Effect of Ws on the performance of the proposed antenna.

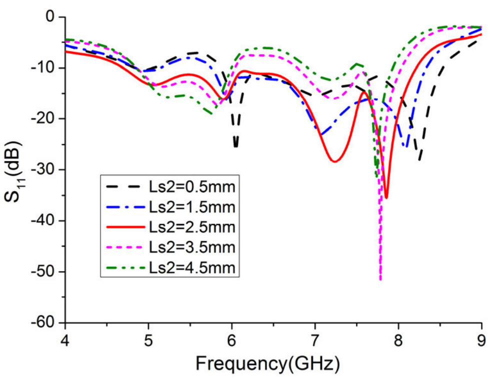

FIGURE 9. Effect of Ls2 on the performance of the proposed antenna.

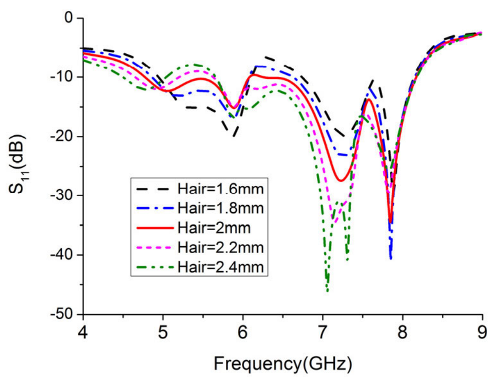

FIGURE 10. Effect of H_{air} on the performance of the proposed antenna.

C. OPTIMIZATION ALGORITHM

In the above discussion, we change one parameter while keeping the other parameters unchanged. In this way, we can study the influence of the different parameters and find an approximately optimal solution. However, all the parameters can be varied simultaneously. To further optimize the parameters, the genetic algorithm (GA) is adopted to obtain the valid performance of the metasurface antenna. The GA tool in MATLAB software with the tournament selection strategy is used. The value of the fitness function in each iteration is taken from the full-wave electromagnetic simulation carried out in the HFSS. Some parameters such as

TABLE 1. Parameters used in the ga optimization.

GA parameter	Value
Population size	200
Number of generations	100
Selection mechanism	Tournament
Cross rate	95%
Mutation rate	5%
Optimization goals	(1)Maximize the impedance bandwidth $\|S_{11}\| = -15dB$; (2) Maximize the 3-dB gain bandwidth

the air height H_{air}, the gap width g, and patch length L_P need to be optimized. Since we want to obtain a good impedance bandwidth and a good gain bandwidth, multi objective optimization is required. The fitness function consists of the impedance bandwidth ($S_{11.BW}$) and the gain bandwidth (G_{BW}) as follows:

$$\text{fitness\_function} = 2 - (w_1 S_{11.BW} + w_2 G_{BW}) \tag{1}$$

with

$$S_{11.BW} = \frac{2(f_{p2} - f_{p1})}{f_{p2} + f_{p1}} \tag{2}$$

$$G_{BW} = \frac{2(f_{up} - f_{down})}{f_{up} + f_{down}} \tag{3}$$

where f_{p2} and f_{p1} are the higher and lower frequencies, respectively, $|S_{11}| = -15dB$, and f_{up} and f_{down} are the higher and lower frequencies, respectively, where the gain decreases by 3 dB compared to the peak gain. We choose $w_1 = w_2 = 0.5$ because both the impedance bandwidth and the gain bandwidth are important. Note that, to improve the resonance of the antenna, we use a more rigorous condition of $|S_{11}| = -15dB$ instead of $|S_{11}| = -10dB$ in the optimization. To achieve the widest gain bandwidth and impedance bandwidth, we expect the fitness function to be positive and minimized. The other parameters used in the GA algorithm for our design are shown in Table 1. The optimized geometrical parameters are as follows: g = 2 mm, $L_P = 9$ mm, and $H_{air} = 2$ mm. After optimization, the impedance bandwidth of the proposed antenna is 54.9% from 4.48–7.87 GHz. In addition, the optimized dimensions are listed in Table 2. Figure 11 shows the simulated S_{11} and gain of the proposed antenna. We can see that the impedance bandwidth is 51.8% from 4.81–8.17 GHz.

D. NONUNIFORM PATCH

From [23], nonuniform metallic patches are used instead of uniform ones to enhanced impedance bandwidth and antenna gain. We know that the radiation element of the traditional patch antenna can be replaced by a periodic array of

TABLE 2. Parameters for the proposed antenna (Unit: mm).

L	Lp	Lf1	Lf2
73	9	37.5	3.5
Lf3	Ls1	Ls2	Wf1
2.5	26	2.5	1.1
Wf2	Ws	θ_1	θ_2
0.8	2	45	25
g	Hair	H	H1
2	2	0.6	1.5

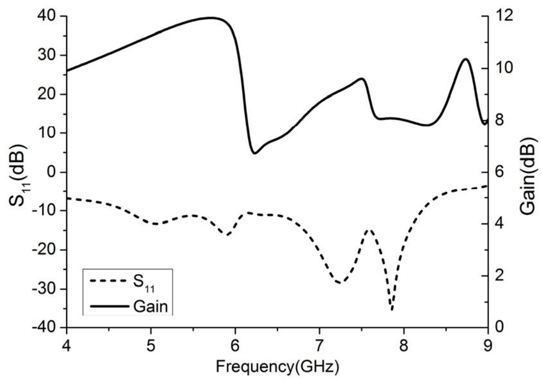

FIGURE 11. Simulated S_{11} and gain of the proposed antenna.

metasurface units loaded with a series capacitor. The proposed metasurface antenna is excited by the aperture coupled structure. In addition, the structure is made of an anomalous microstrip line and a narrow slot etched in the ground plane. The surface current density of the antenna at 7.25 GHz is shown in Figure 12. We can see that the surface current density on the copper patch array is mostly concentrated in the center cells. The surface currents on the marginal cells are obviously weaker because of the long distance from the coupling slot. Therefore, the marginal cells are hardly excited simultaneously with the center cells. The amplitude is related to both the frequency and the phase distribution. The current distribution is strongly related to the resonance of the patch array, as the array's dimension is comparable with the wavelength at operation frequencies. The patches in the bottom-left and top-right corners might carry the strongest current due to phase cancellation and addition. The distance between them may cause reversed-phase addition; thus, it carries the strongest current. Nonuniform metallic patch cells are added to improve the uniformity of the antenna array. Finally, the gain is improved.

To address this shortcoming, the metasurface antenna is modified with nonuniform patch (NP), as shown in Figure 13. Both array surfaces are modified. We introduce PE along the E-plane periphery. The marginal cells in the upper metal layer of the metasurface are extended lengthwise along the x-axis and y-axis, and the other parameters are unchanged. The effects of the extended length H_{cd} on the antenna are studied and shown in Figure 14 and Figure 15. We can see that, when H_{cd} = 1.5 mm, the gain of the antenna is high and the impedance bandwidth is the widest.

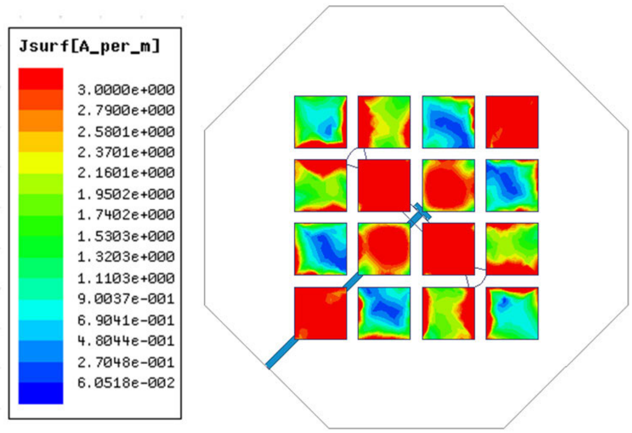

FIGURE 12. Simulated surface current density of the antenna.

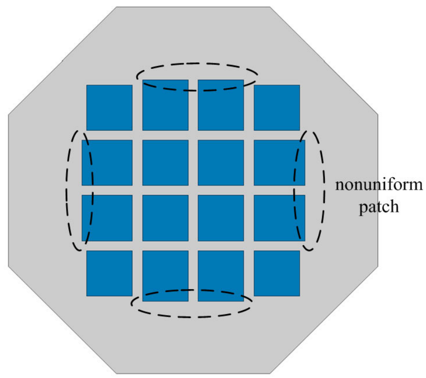

FIGURE 13. Modified antenna with the nonuniform patch.

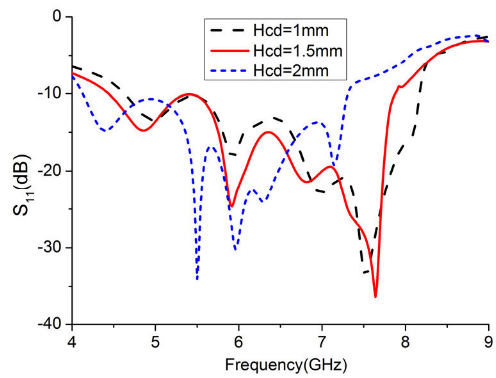

FIGURE 14. Simulated S_{11} of the modified antennas with different H_{cd}.

Figure 16 shows the simulated S_{11} and gain of the antenna without and with PE. We can see clearly that the gain of the modified antenna with PE is better than that of the primary antenna. The gain of the modified antenna increased by over 1.5 dBi at 6.1 GHz. The gain from 6–7.3 GHz increased by over 1 dBi on average. The impedance bandwidth exhibits little change. As a result, the amplitude of the surface current in the marginal cells is perturbed but relatively uniform, as shown in Figure 17, which illustrates that PE enlarges

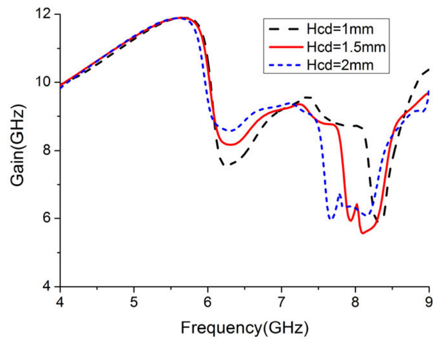

FIGURE 15. Simulated gain of the modified antennas with different H_{cd}.

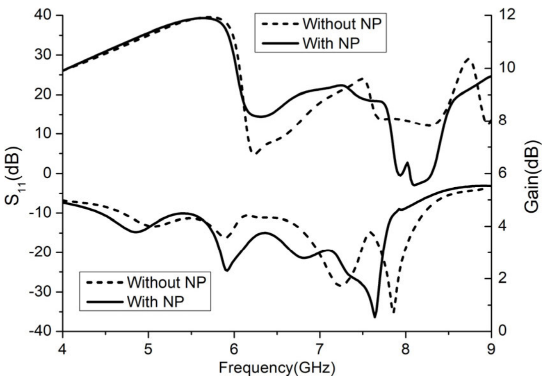

FIGURE 16. Simulated S_{11} and gain of the antennas with and without the nonuniform patch.

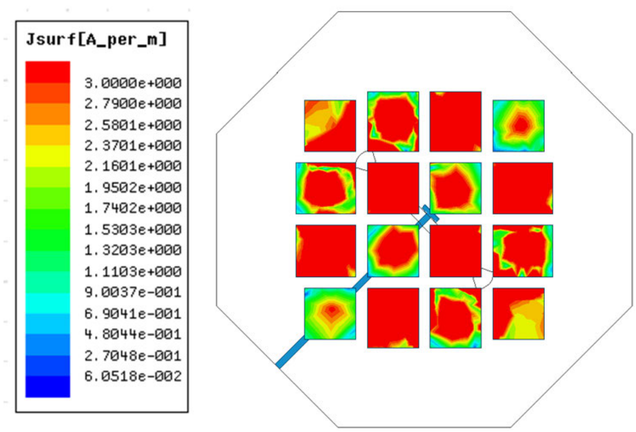

FIGURE 17. Simulated surface current density of the modified antenna.

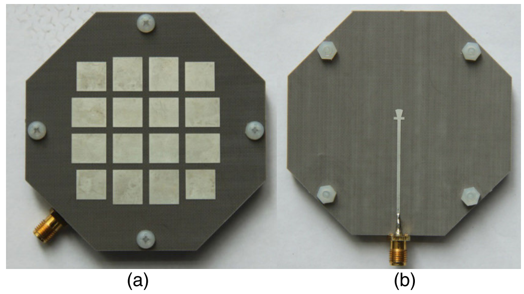

FIGURE 18. Photographs of the proposed antenna. (a) Top view of the metasurface. (b) Top view of the feeding layer.

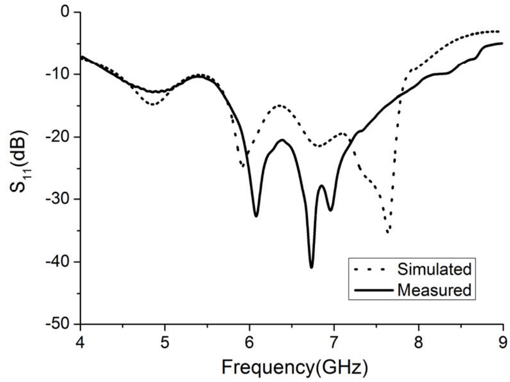

FIGURE 19. Simulated and measured S_{11} of the modified antenna.

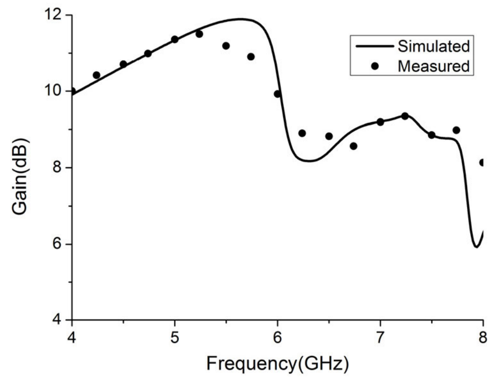

FIGURE 20. Simulated and measured gain of the modified antenna.

the effective radiation and enhances the gain of the antenna effectively.

III. EXPERIMENTAL RESULTS AND DISCUSSION OF THE PROPOSED ANTENNA

To validate the design, the proposed metasurface antenna is fabricated as shown in Figures 18 (a) and (b). The S_{11} of the antenna is measured with an AV 3672B vector network analyzer and is shown in Figure 19. It is found that the 10-dB impedance bandwidth ranges from 4.48 GHz to 7.87 GHz (54.9%). The gain and the radiation pattern are measured in an anechoic chamber. Figure 20 shows the measured gain of the modified antenna, which agrees well with the simulated results. Figure 21 shows the radiation efficiency of the antenna. The measured efficiency is slightly lower than the simulated data, mainly due to the transition loss of the SMA connector and a small assembling offset of multilayer substrates. The measured E-plane and H-plane radiation patterns at four representative frequencies, 4.84, 5.91, 7.25, and 7.86 GHz, in the working band are shown in Figure 22. Good agreement is obtained between the simulated and measured results. It can be seen that desirable broadside radiations are obtained at all three frequency points.

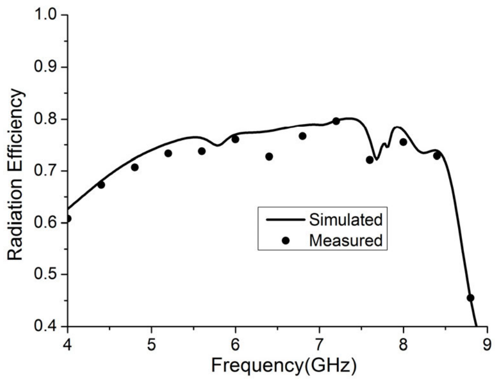

FIGURE 21. Simulated and measured radiation efficiency of the modified antenna.

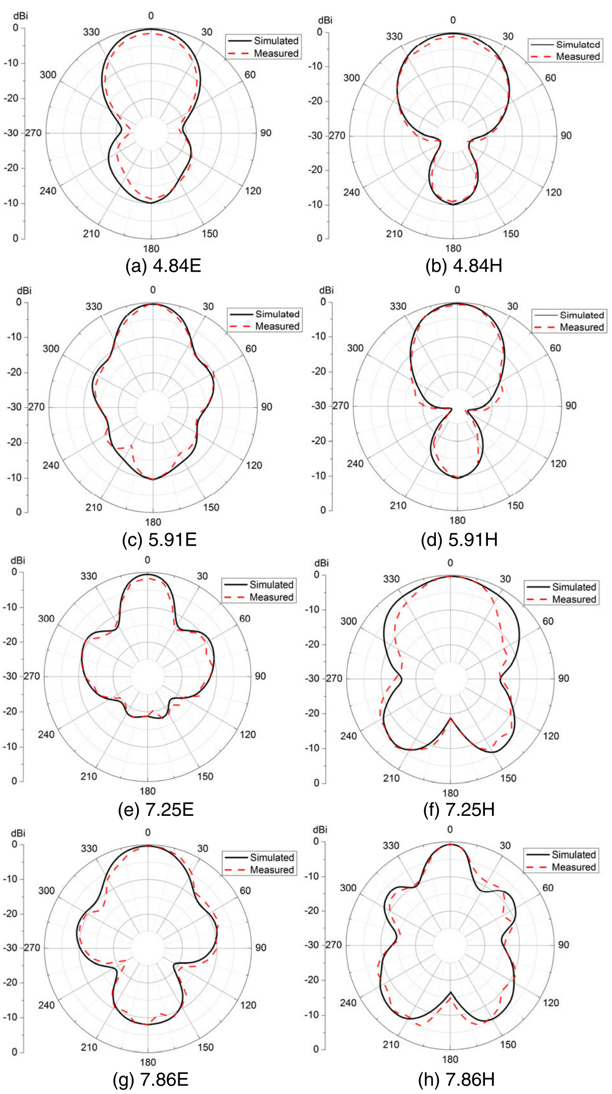

FIGURE 22. Simulated and measured radiation patterns of the proposed antenna.

IV. CONCLUSION

In this paper, a wideband low-profile high-gain metasurface antenna is proposed. The metasurface consists of two stacking layers and a ground plane. In addition, the metasurface antenna is excited by an aperture coupled structure that is placed underneath the metasurface. We adopt GA to obtain the valid performance of the metasurface antenna. The gain is enhanced by introducing nonuniform patch while keeping the other parts of the antenna fixed. The measured results indicate that the proposed antenna has high gain with low profile.

REFERENCES

[1] J.-J. Liang, G.-L. Huang, J.-N. Zhao, Z.-J. Gao, and T. Yuan, "Wideband phase-gradient metasurface antenna with focused beams," *IEEE Access*, vol. 7, pp. 20767–20772, 2019.
[2] F. H. Lin and Z. N. Chen, "Low-profile wideband metasurface antenna using characteristic mode analysis," *IEEE Trans. Antennas Propag.*, vol. 65, no. 4, pp. 1706–1713, Apr. 2017.
[3] J. Zhu, S. Liao, S. Li, and Q. Xue, "60 GHz wideband high-gain circularly polarized antenna array with substrate integrated cavity excitation," *IEEE Antennas Wireless Propag. Lett.*, vol. 17, no. 5, pp. 751–755, May 2018.
[4] Z. Shen and C. Feng, "A new dual-polarized broadband horn antenna," *IEEE Antennas Wireless Propag. Lett.*, vol. 4, pp. 270–273, Aug. 2005.
[5] M. K. T. Al-Nuaimi, W. Hong, and Y. Zhang, "Design of high-directivity compact-size conical horn lens antenna," *IEEE Antennas Wireless Propag. Lett.*, vol. 13, pp. 467–470, 2014.
[6] M. Liang, W. R. Ng, K. Chang, K. Gbele, M. E. Gehm, and H. Xin, "A 3-D Luneburg lens antenna fabricated by polymer jetting rapid prototyping," *IEEE Trans. Antennas Propag.*, vol. 62, no. 4, pp. 1799–1807, Apr. 2014.
[7] E. Erfani, M. Niroo-Jazi, and S. Tatu, "A high-gain broadband gradient refractive index metasurface lens antenna," *IEEE Trans. Antennas. Propag.*, vol. 64, no. 5, pp. 1968–1973, May 2016.
[8] H. Li, G. Wang, H.-X. Xu, T. Cai, and J. Liang, "X-band phase-gradient metasurface for high-gain lens antenna application," *IEEE Trans. Antennas Propag.*, vol. 63, no. 11, pp. 5144–5149, Nov. 2015.
[9] Y. Li, Z. Zhang, C. Deng, Z. Feng, and M. F. Iskander, "2-D planar scalable dual-polarized serious-fed slot antenna srrsy using single substrate," *IEEE Trans. Antennas Propag.*, vol. 62, no. 4, pp. 2280–2283, Apr. 2014.
[10] J.-J. Liang, G.-L. Huang, and J.-N. Zhao, "Novel parasitic microstrips arrays for low-cost active phased array applications," *IEEE Trans. Antennas Propag.*, vol. 62, no. 4, pp. 1731–1737, Apr. 2014.
[11] W. Yang, S. Chen, W. Che, Q. Xue, and Q. Meng, "Compact high-gain metasurface antenna arrays based on higher-mode SIW cavities," *IEEE Trans. Antennas Propag.*, vol. 66, no. 9, pp. 4918–4923, Sep. 2018.
[12] W. Liu, Z. N. Chen, and X. Qing, "Metamaterial-based low-profile broadband aperture-coupled grid-slotted patch antenna," *IEEE Trans. Antennas Propag.*, vol. 63, no. 7, pp. 3325–3329, Jul. 2015.
[13] S.-X. Ta and I. Park, "Low-profile broadband circularly polarized patch antenna using metasurface," *IEEE Trans. Antennas Propag.*, vol. 63, no. 12, pp. 5929–5934, Dec. 2015.
[14] Z. Wu, L. Li, Y. Li, and X. Chen, "Metasurface superstrate antenna with wideband circular polarization for satellite communication application," *IEEE Antennas Wireless Propag. Lett.*, vol. 15, pp. 374–377, 2016.
[15] C. L. Holloway, E. F. Kuester, J. A. Gordon, J. O'Hara, J. Booth, and D. R. Smith, "An overview of the theory and applications of metasurfaces: The two-dimensional equivalents of metamaterials," *IEEE Antennas Propag. Mag.*, vol. 54, no. 4, pp. 10–35, Jul. 2012.
[16] X. Ni, N. K. Emani, A. V. Kildishev, A. Boltasseva, and V. M. Shalaev, "Broadband light bending with plasmonic nanoantennas," *Science*, vol. 335, no. 6067, p. 427, Jan. 2012.
[17] Y. F. Li, "Wideband radar cross section reduction using two-dimensional phase gradient metasurfaces," *Appl. Phys. Lett.*, vol. 104, no. 22, p. 1, Jun. 2014.
[18] J. Cheng and H. Mosallaei, "Optical metasurfaces for beam scanning in space," *Opt. Lett.*, vol. 39, no. 9, pp. 2719–2722, May 2014.
[19] B. Majumder, K. Kandasamy, and J. Mukherjee, "Wideband compact directive metasurface enabled pair of slot antennas," *Electron. Lett.*, vol. 51, no. 17, pp. 1310–1312, 2015.
[20] W. Liu, Z. N. Chen, and X. Qing, "Metamaterial-based low-profile broadband mushroom antenna," *IEEE Trans. Antennas Propag.*, vol. 62, no. 3, pp. 1165–1172, Mar. 2014.

[21] Z. Z. Yang, F. Liang, Y. Y. D. Zhao, and B. Z. Wang, "Metasurface-based wideband, low-profile, and high-gain antenna," *IET Microw., Antennas Propag.*, vol. 13, no. 4, pp. 436–441, 2019.
[22] W. J. Yang, Y. M. Pan, and S. Y. Zheng, "A low-profile wideband circularly polarized crossed-dipole antenna with wide axial-ratio and gain beamwidths," *IEEE Trans. Antennas Propag.*, vol. 66, no. 7, pp. 3346–3353, Jul. 2018.
[23] Y. M. Pan, P. F. Hu, X. Y. Zhang, and S. Y. Zheng, "A low-profile high-gain and wideband filtering antenna with metasurface," *IEEE Trans. Antennas Propag.*, vol. 64, no. 5, pp. 2010–2016, May 2016.

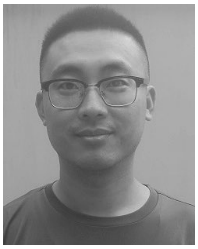

HAO BAI was born in China, in 1987. He received the B.S. and M.S. degrees in electromagnetic field and microwave technology from Xidian University, Xi'an, China, in 2009 and 2014, respectively. He is currently pursuing the Ph.D. degree with Air Force Engineering University. His research interests include antenna array, antenna decoupling technology, and metasurfaces.

GUANG-MING WANG was born in China, in 1964. He received the B.S. and M.S. degrees from Air Force Engineering University, Xi'an, China, in 1982 and 1990, respectively, and the Ph.D. degree from the University of Electronic Science and Technology, Chengdu, China, in 1994, all in electromagnetic field and microwave technology.

He joined Air Force Engineering University as an Associate Professor and promoted to a Full Professor, in 2000, where he is currently the Head of the Microwave Laboratory. He has authored or coauthored more than 100 conference and journal articles. His current interests include microwave circuits, antennas, and new structures, including EBG, PBG, metamaterials, and fractals.

Prof. Wang has been a Senior Member of the Chinese Commission of Communication and Electronic. Since 1994, he has been awarded and warranted several items supported under the National Natural Science Foundation of China and fulfilled many local scientific research programs.

TING WU was born in China, in 1987. She received the B.S. and Ph.D. degrees in electromagnetic field and microwave technology from Xidian University, Xi'an, China, in 2009 and 2016, respectively. She is currently working with the Xi'an University of Technology. Her research interests include antenna array and metasurfaces.